ARCHIVES OF ELECTRICAL ENGINEERING VOL. 62(3), pp. 449-461 (2013)

DOI 10.2478/aee-2013-0036

Cogging torque sensitivity to permanent magnet tolerance combinations*

LOVRENC GAŠPARIN[1], RASTKO FIŠER[2]

[1]*Letrika d.d., Polje 15, 5290 Šempeter pri Gorici, Slovenia*
e-mail: Lovrenc.Gasparin@letrika.com

[2] *Faculty of Electrical Engineering, University of Ljubljana*
Tržaška cesta 25, 1000 Ljubljana, Slovenia
e-mail: Rastko.Fiser@fe.uni-lj.si

(Received: 26.06.2012, revised: 10.12.2012)

Abstract: This study presents the dependence of the level and harmonic structure of the cogging torque in permanent magnet synchronous motors (PMSM) to imperfections of permanent magnet (PM) dimensions and positions, which can not be avoided in mass-production. Slightly diverse dimensions and misplacements of PMs are introducing asymmetries in magnetic field distribution which cause additional harmonic components. A finite element method (FEM) and Fast Fourier transform (FFT) were used to calculate cogging torque harmonic components with regard to several combinations of PM assembly imperfections. It has been established and proved that unequal PMs cause magnetic asymmetries which give rise to additional cogging torque harmonic components and consequently increase the total cogging torque. It is also shown that in some particular combinations the influence of an individual PM imprecision could compensate with others due to different phase shifts which can result even in the decrease of cogging torque. Considering presented results it is possible to foresee which additional harmonic components will comprise the cogging torque of mass-produced PMSMs due to PM imperfections. In this way the designers are able to predetermine required manufacturing tolerances to keep the level of cogging torque in a admissible level. Simulation results were verified and confirmed by laboratory tests.

Key words: cogging torque, finite element method, harmonic components, PM synchronous motor

1. Introduction

High-performance drives in automotive applications require permanent magnet synchronous motors (PMSM) that produce smooth torque with a very low component of cogging torque. This is not easy to attain as improper designs of PMSMs result in cogging torque that may be inadmissibly high regarding the rated torque. In lower cost machines, it has typically

* This is extended version of a paper which was presented at the 22th *Symposium on Electromagnetic Phenomena in Nonlinear Circuits*, Pula, Croatia, 26.06-29.06 2012.

value around 5% of the rated torque [1, 2]. As nowadays number of high-performance applications necessitate cogging torque not to exceed 1% of the rated torque, effective methods for its analysis and computation are required to design machines that meet such specifications [3, 4]. Minimization of cogging torque frequently becomes a challenging task, since it is composed of numerous harmonic components, which originate in combination of many design parameters and material or assembly imperfections [5-7]. Besides applying appropriate combination of stator and rotor design techniques [5, 8-10, 17-19], the other option for cogging torque reduction is to introduce advanced control methods of the drive [11]. Regularly observed substantial differences between calculated (simulated) and measured cogging torque values was a cogent motive for the presented research of cogging torque sensitivity to manufacturing imperfections and tolerances, which are unavoidable facts in mass-production.

2. Harmonic components of cogging torque

Total cogging torque T_{cog} of PMSM is composed of several harmonic components, which can be classified into two groups [6, 12]. The first group represents an array of "native" harmonic components T_{NHC} which originate in a combination of design parameters, mostly the number of stator slots Q and the number of rotor magnetic poles P. The second group is an array of "additional" harmonic components T_{AHC}, which are the consequence of material and assembly imperfections and would not be present in the case of a hypothetical perfectly manufactured motor [13, 14]. Each harmonic component could be described by the following parameters: an amplitude A, an order (number of repetitions in mechanical revolution) N, φ stands for a phase shift. Native harmonic components T_{NHC} have orders defined by expression (4). Additional harmonic components T_{AHC} can be further classified as contributions of imperfections which originate either on the stator or rotor side. In this paper only the case of rotor permanent magnet (PM) imperfections will be presented, where the orders of such T_{AHC} are defined by expressions (5).

$$T_{cog}(\alpha) = T_{NHC}(\alpha) + T_{AHC}(\alpha), \tag{1}$$

$$T_{NHC}(\alpha) = \sum_{i=1}^{\infty} A_{NHC\,i} \cdot \sin\left(N_{NHC\,i} \cdot \alpha + \varphi_{NHC\,i}\right), \tag{2}$$

$$T_{AHC}(\alpha) = \sum_{i=1}^{\infty} A_{AHC\,i} \cdot \sin\left(N_{AHC\,i} \cdot \alpha + \varphi_{AHC\,i}\right), \tag{3}$$

$$N_{NHCi} = \mathrm{LCM}(Q, P) \cdot i, \tag{4}$$

$$N_{NHCi} = Q \cdot i. \tag{5}$$

3. FEM model of PMSM

PMSM with $Q = 9$ and $P = 6$ (cross-section shown in Fig. 1a), which is manufactured in mass-production with demand for extremely low level of cogging torque (T_{cog} less than 9 mNm whereas the nominal torque is 4.5 Nm) has been parametrically modeled. Regarding equations (4) and (5), for this particular PMSM design first three expected harmonic orders are $N_{NHC\,i} = 18$, 36, 54, and $N_{AHC\,i} = 9$, 18, 27, respectively. Rotor consists of 6 PMs (Fig. 1c), which in general have slightly diverse dimensions (thickness, width, radii) due to production tolerances. Simulation FEM model has been prepared in a way that for each individual PM all 7 dimensions can be varied independently with the following parameters (Fig. 1d):

- a, f – PM width,
- b, e – left and right PM edge thickness,
- c – thickness at the centre of PM,
- d – misalignment of outer PM radius,
- g – PM position on rotor core.

In one rotor group there are 6 PMs for a chosen motor design, which gives a total amount of 42 parameters. To reduce native harmonic components of T_{cog} a well-known design technique of a PM step-skew has been considered [8], thus additional parameter that can deviate from exact value is also a step-skew angle θ (Fig. 1b). On actual rotor there are 3 groups of PMs, each group skewed for $\theta = 6.66$ °. It is not necessary to develop a 3D FEM model for cogging torque calculation, as it can be calculated with three 2D FEM parametric models for each group separately. The Ansys software has been used for a 2D FEM parametric model and LabView for summation of three cogging torque signals (for three groups) and for FFT analyses.

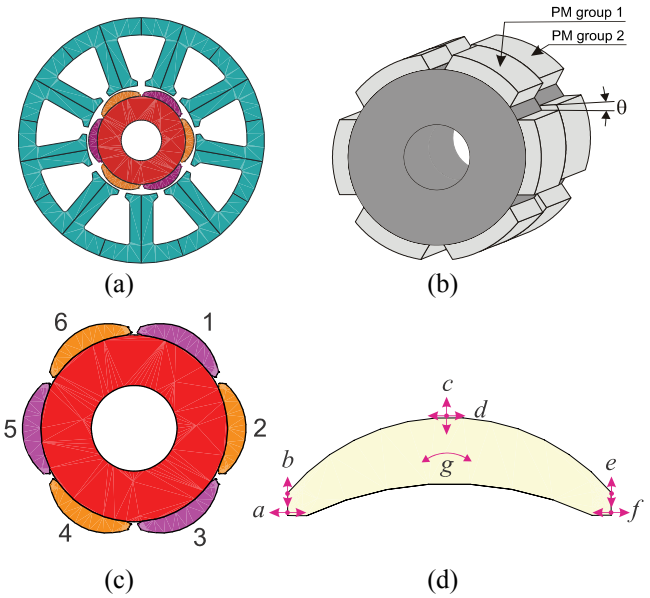

Fig. 1. Geometry of the PMSM (a), step-skew of 2 PM groups (c), rotor with 6 PMs (c), variable PM parameters of FEM model (d)

4. FEM calculations and simulation results

In one group of 6 PMs there are 42 variables, thus to model one rotor with step-skew of 2 groups there are 84 variables and additional one for a step-skew misalignment. For the case of 3 step-skew PM groups, which more intensively reduce $T_{NHC\,i}$, there is a total of 128 variables. Each variable has a prescribed tolerance which depends on applied mass-production technology, thus analyzing each possible permutation is practically unfeasible. Furthermore, with so many parameters and combinations understandable picture of their influence on the cogging torque level can easily be misled. For that reason we initially studied only combinations of PM positioning (parameter g in Fig. 1d), other parameters were in presented study the same and ideal for all 6 PMs in one group.

Modeled assembly imperfection – misalignment of 1 PM

In the first presented case there is one PM misaligned from ideal position for +0.3°, all others five are perfectly aligned. There are 6 such possible combinations (Tab. 1), where misaligned PM is marked with number 1 and ideally positioned PMs are denoted as 0. Six models and six calculated cogging torque signals result in only two different T_{cog} characteristics (Fig. 2). Combinations 1, 3, 5 (marked as green) represent misaligned south PMs, while combinations 2, 4, 6 (marked as yellow) stand for north PMs, which are misplaced from symmetrical position due to assembly imperfections. Combination 0 corresponds to the case of ideal position of all 6 PMs (blue curve).

Table 1. Possible combinations of 1 PM misaligned from ideal position

Comb.	PM 1	PM 2	PM 3	PM 4	PM 5	PM 6
0	0	0	0	0	0	0
1	0	0	0	0	0	1
2	0	0	0	0	1	0
3	0	0	0	1	0	0
4	0	0	1	0	0	0
5	0	1	0	0	0	0
6	1	0	0	0	0	0

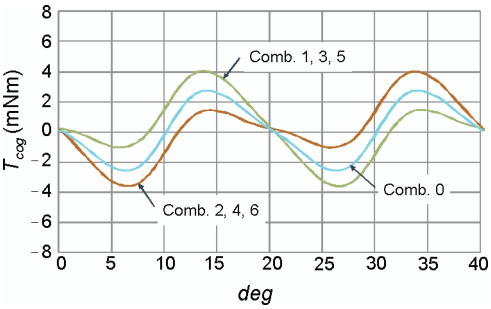

Fig. 2. Calculated T_{cog} for a perfect rotor and 6 possible misalignments of 1 PM

Examination of calculated T_{cog} for Comb. 1, 3, 5 and Comb. 2, 4, 6 (Table 1) clearly show that signals are phase shifted for 20° in mechanical revolution (Fig. 2) indicating that some

T_{AHC} components are having different phase shifts. FFT analysis shows for Comb. 0 (initial case of perfectly aligned all 6 PMs) harmonic orders $N_{NHC\,1} = 18$ and $N_{NHC\,2} = 36$, which correspond to expression (4). Their amplitude values are $A_{NHC\,1} = 2.44$ mNm and $A_{NHC\,2} = 0.51$ mNm (Fig. 3), and corresponding phase shifts are $\varphi_{NHC\,1} = +90°$ and $\varphi_{NHC\,2} = -90°$ (Fig. 4).

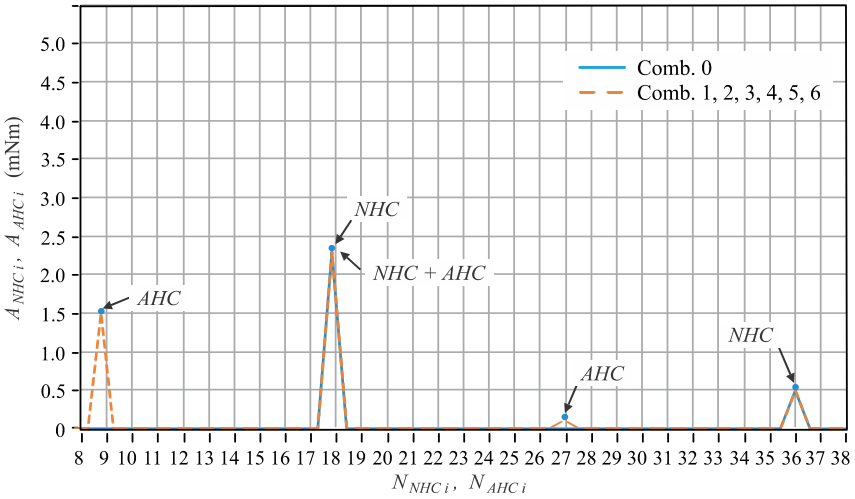

Fig. 3. FFT of calculated T_{cog} – amplitude values for all 7 combinations of 1 PM misplacement

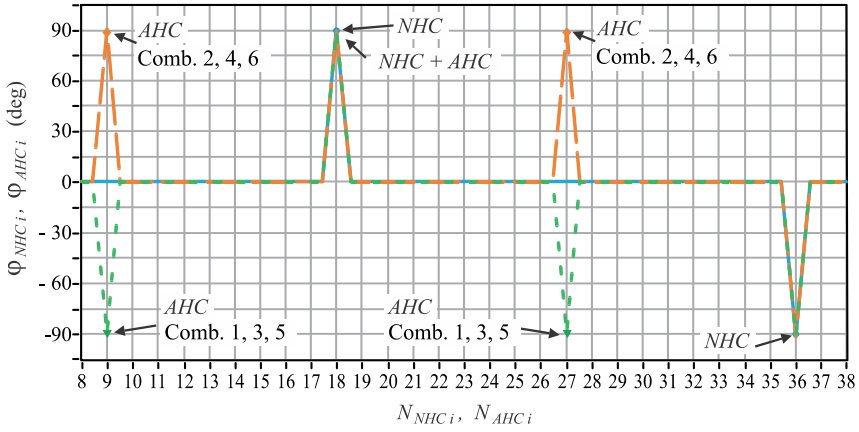

Fig. 4. FFT of calculated T_{cog} – phase shifts for all 7 combinations of 1 PM misplacement

Further analysis of FFT spectrum reveals additional harmonic orders $N_{AHC\,1} = 9$ and $N_{AHC\,3} = 27$ with amplitude values $A_{AHC\,1} = 1.58$ mNm and $A_{AHC\,3} = 0.10$ mNm (Fig. 3). In this case 18th harmonic order is shared between $N_{NHC\,1}$ and $N_{AHC\,2}$ (eq. (4) and (5)), with amplitude value of $A_{NHC\,1+AHC\,2} = 2.46$ mNm. Compared to the case of all 6 PMs perfectly aligned

($A_{NHC\,1}$ = 2.44 mNm), the difference is only 0.02 mNm. For all 6 combinations of misaligned 1 PM amplitude values are the same (Fig. 3).

Detailed FFT analysis of T_{cog} discloses also that phase shifts for Comb. 1, 3, 5 are $\varphi_{AHC\,1} = -90°$ and $\varphi_{AHC\,3} = -90°$, while for Comb. 2, 4, 6 are $\varphi_{AHC\,1} = +90°$ and $\varphi_{AHC\,3} = +90°$ (Fig. 4). As seen phase shift difference between Comb. 1, 3, 5 and Comb. 2, 4, 6 is 180°, which causes shift of 20° in mechanical revolution of calculated T_{cog} (Fig. 2). For shared harmonic order phase shift is $\varphi_{NHC\,1+AHC\,2} = +90°$ for all combinations.

Modeled assembly imperfection – misalignment of 2 PM

In the second case we have considered every possible combinations for two PMs misaligned from ideal positions and other four PMs are perfectly placed (Tab. 2). Among all 15 combinations only 3 different calculated cogging torque signals were obtained (Fig. 5). Moreover, there are 6 combinations with the presence of T_{AHC} due to PM misplacements, while other 9 potential combinations produce no T_{AHC} at all, which means that some particular combinations of imperfections are compensating, thus not all of them reflect in the same manner and intensity. Amplitude values of T_{cog} have increased compared to the first case, where only 1 PM was misaligned and the asymmetry was less expressed. The case of ideal assembled rotor is the same as shown in Figure 2 (blue curve) and therefore omitted in further analysis.

Table 2. Possible combinations of 2 PMs misaligned from ideal positions

Comb.	PM 1	PM 2	PM 3	PM 4	PM 5	PM 6
1	0	0	0	0	1	1
2	0	0	0	1	0	1
3	0	0	0	1	1	0
4	0	0	1	0	0	1
5	0	0	1	0	1	0
6	0	0	1	1	0	0
7	0	1	0	0	0	1
8	0	1	0	0	1	0
9	0	1	0	1	0	0
10	0	1	1	0	0	0
11	1	0	0	0	0	1
12	1	0	0	0	1	0
13	1	0	0	1	0	0
14	1	0	1	0	0	0
15	1	1	0	0	0	0

In depth analysis of T_{cog} using FFT discovers additional harmonic orders $N_{AHC\,1} = 9$ and $N_{AHC\,3} = 27$, which are the same as in previous case of 1 misaligned PM but with doubled

amplitude values $A_{AHC\,1} = 3.16$ mNm and $A_{AHC\,3} = 0.20$ mNm (Fig. 6). Again, the 18th harmonic order component is shared between $N_{AHC\,2}$ and $N_{NHC\,1}$, with amplitude value of $A_{NHC\,1+AHC\,2} = 2.48$ mNm. Compared to the case of all 6 PM perfectly aligned ($A_{NHC\,1} = 2.44$ mNm in Fig. 3) the difference is only 0.08 mNm, which proves that it remains practically the same.

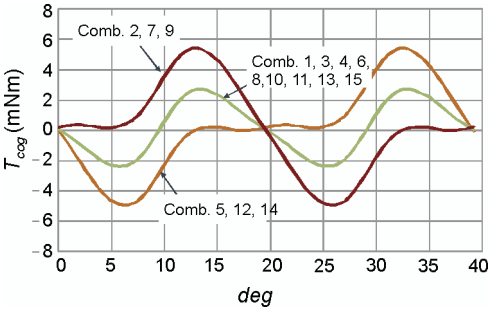

Fig. 5. Calculated T_{cog} for all 15 possible misalignments of 2 PMs

For 6 combinations (Comb. 2, 7, 9, 5, 12, 14) amplitude values are equal and for all remaining 9 combinations, where imperfections are compensating, there are observed no T_{AHC}, moreover calculated $A_{NHC\,1} = 2.44$ mNm is equal as in the case of perfectly aligned all 6 PMs (Fig. 6). Which combinations increases T_{AHC} and consequently T_{cog} the most can easily be noticed in Table 2 and Fig. 5. Phase shifts for Comb. 5, 12, 14 are $\varphi_{AHC\,1} = +90°$ and $\varphi_{AHC\,3} = +90°$, while for Comb. 2, 7, 9 are $\varphi_{AHC\,1} = -90°$ and $\varphi_{AHC\,3} = -90°$ (Fig. 7). Phase shifts actually determine how PM dimension irregularities are contributing to the total T_{cog}. In case of Comb. 2, 7, 9, 5, 12, 14 phase shifts are equal as in the case of perfectly aligned all 6 PMs.

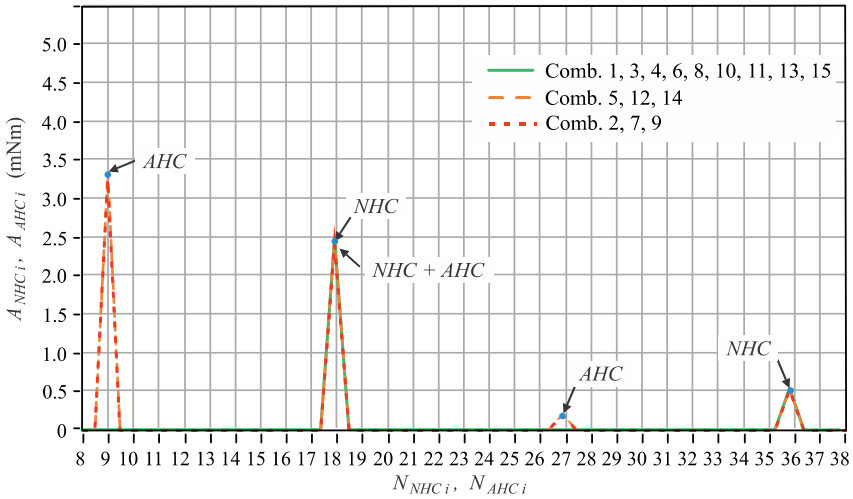

Fig. 6. FFT of calculated T_{cog} – amplitude values for all 15 combinations of 2 PMs misplacements

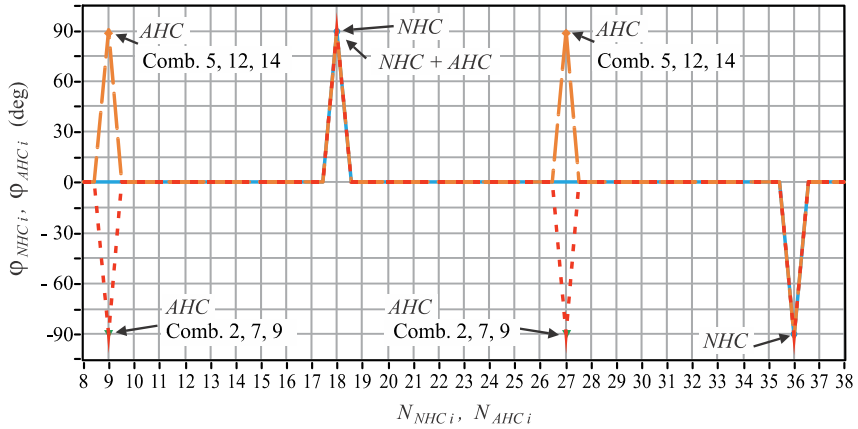

Fig. 7. FFT of calculated T_{cog} – phase shifts for all 15 combinations of 2 PMs misplacements

Modeled assembly imperfection – misalignment of 3 PM

In the third case were considered potential combinations for three PMs misaligned for +0.3° from ideal position, while remaining three PMs are perfectly aligned (Table 3).

Table 3. Possible combinations of 3 PMs misaligned from ideal positions

Comb.	PM 1	PM 2	PM 3	PM 4	PM 5	PM 6
1	0	0	0	1	1	1
2	0	0	1	0	1	1
3	0	0	1	1	0	1
4	0	0	1	1	1	0
5	0	1	0	0	1	1
6	0	1	0	1	0	1
7	0	1	0	1	1	0
8	0	1	1	0	0	1
9	0	1	1	0	1	0
10	0	1	1	1	0	0
11	1	0	0	0	1	1
12	1	0	0	1	0	1
13	1	0	0	1	1	0
14	1	0	1	0	0	1
15	1	0	1	0	1	0
16	1	0	1	1	0	0
17	1	1	0	0	0	1
18	1	1	0	0	1	0
19	1	1	0	1	0	0
20	1	1	1	0	0	0

Among all 20 combinations there are only 4 different calculated T_{cog} signals (Fig. 8). Examples 6 and 15 are extremely high in amplitude values in comparison to previous analyzed cases, while for all other combinations amplitudes are similar as in cases of 1 misplaced PM.

Fig. 8. Calculated T_{cog} for all 20 possible misalignments of 3 PMs

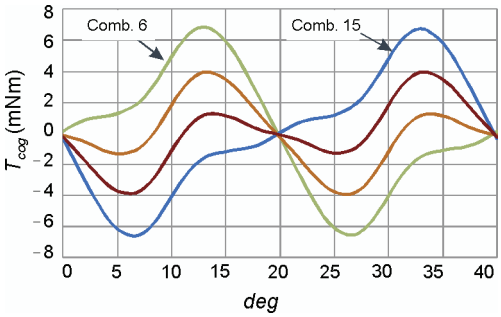

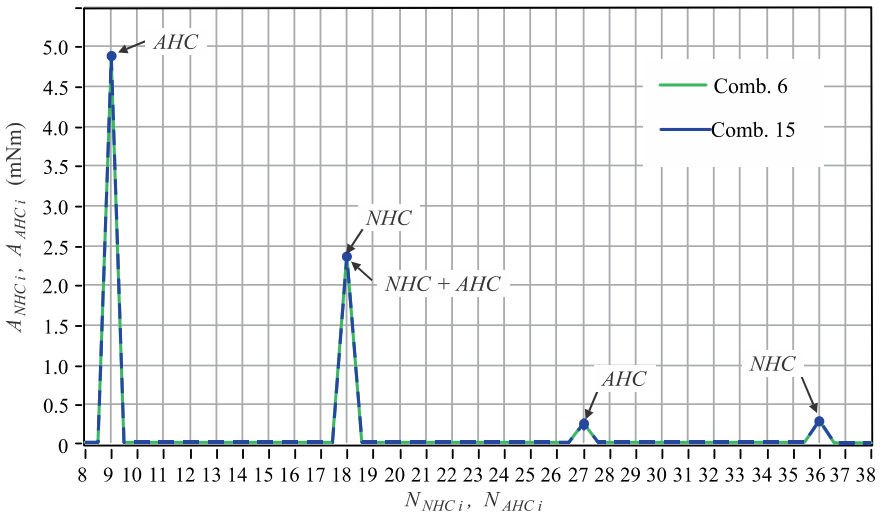

Fig. 9. FFT of calculated T_{cog} – amplitude values for Comb. 6 and Comb. 15

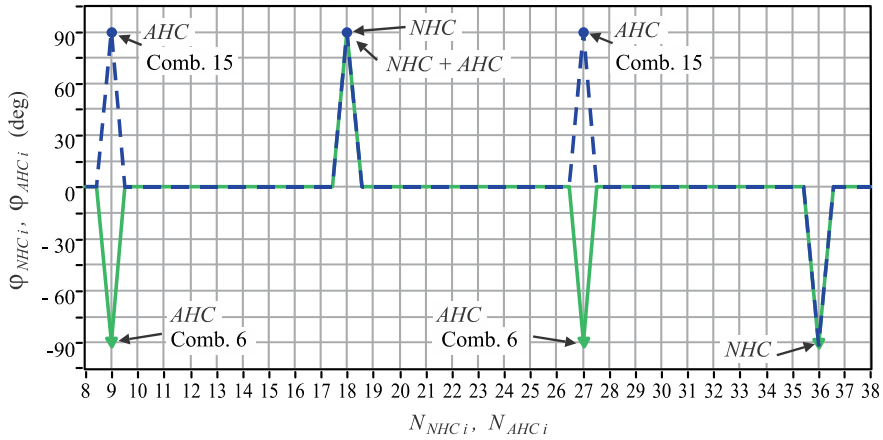

Fig. 10. FFT of calculated T_{cog} – phase shifts for Comb. 6 and Comb. 15

FFT cogging torque analysis ascertains additional harmonic orders $N_{AHC\,1} = 9$, $N_{AHC\,3} = 27$, the same as in all previous cases, but with triple amplitude values compared to a case of 1 misaligned PM: $A_{AHC\,1} = 4.74$ mNm and $A_{AHC\,3} = 0.30$ mNm (Fig. 9). Phase shifts for Comb. 15 is $\varphi_{AHC\,1} = +90°$ and $\varphi_{AHC\,3} = +90°$, while for Comb. 6 are $\varphi_{AHC\,1} = -90°$ and $\varphi_{AHC\,3} = -90°$ (Fig. 10), similar to the case of 1 and 2 misaligned PM.

5. Experimental results

As already described, rotor under test consist of 18 PMs divided into 3 groups of 6 PMs (Fig. 11). Step-skew between groups is 6.66° to reduce existing $N_{NHC\,1} = 18$ and $N_{NHC\,2} = 36$ components. Preliminary sorting of PMs is necessary to assemble prototype rotor with as much as possible equal PMs like modeled in FEM simulations. PMs were sorted by width (parameters *a*, *f* in Fig. 1d), thickness at the centre (*c*), and left and right edge thickness (*b*, *e*), respectively.

Fig.11. Assembled rotor with 3 step-skew groups of 6 PMs

To verify presented FEM model and to confirm theoretical considerations, we fabricated several rotor samples. To prove how slight variations in geometry, which at first sight seems negligible, can influence the T_{cog}, we assembled a rotor with 6 PMs, which have thickness at the right edge for 0.1 mm higher compared to the thickness of the left edge, 3 PMs having thickness difference at the right edge of 0.05 mm and 9 PMs with ideal dimensions (Fig. 12). Such chosen combination gave the worst result denoted as Comb. 15 in the case of 3 dissimilar PMs (Table 3, Fig. 8 and 10). The same distribution of dissimilar PMs has also been applied in FEM simulation model.

FFT of calculated and measured T_{cog} are compared in Figure 13. In analysis a frequency spectrum of T_{cog} gives us much better, more detailed insight and clear information on cogging torque origins as representation in the means of T_{cog} waveforms versus time or geometrical angle (like in Figs. 2, 5, 8) due to very demanding and sensitive measurement procedure, which needs additional advanced filtering and processing to eliminate several external disturbances [12].

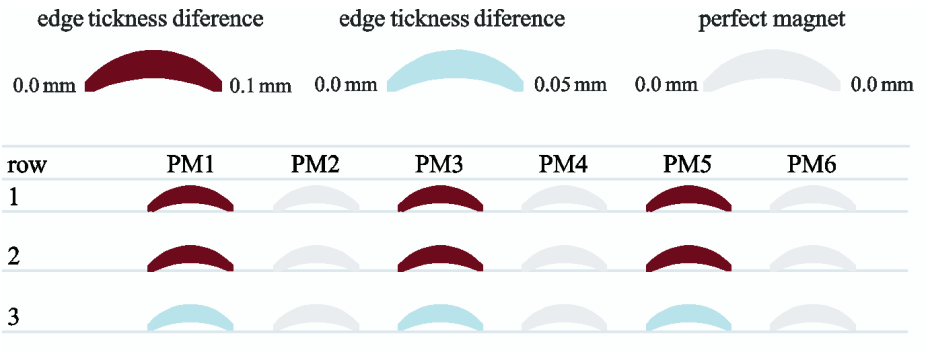

Fig. 12. PMs distribution on a prototype rotor

FFT analysis clearly shows the presence of $N_{AHC\,1} = 9$ in both, measured and calculated T_{cog}. Amplitude value of calculated is $A_{AHC\,1} = 7.19$ mNm, whereas measured is $A_{AHC\,1} = 6.40$ mNm. The difference is 12.3%, which is acceptable discrepancy knowing that cogging torque is very sensible to the smallest deviations of PM dimensions. Such small differences in geometry are also very difficult to measure accurately. It can be observed that the measured amplitude of $N_{NHC\,1} = 18$ harmonic order is much higher than the calculated one. It is due to the fact that the step-skew angle θ was not exactly 6.66°, as we found out later by precise measurements. In measured T_{cog} can be seen some other harmonic components $N_{AHC\,i} = 6$, 12, 18 that are correlated to asymmetries in a stator lamination stack like interlocks and notches [12, 15]. Another parameter, which was not considered in presented study but certainly exists, is a discrepancy in PM magnetization [16], anyway this effect has origin on the rotor side, therefore it contributes T_{AHC} components of already known orders $N_{AHC\,i} = 9$, 18, 27.

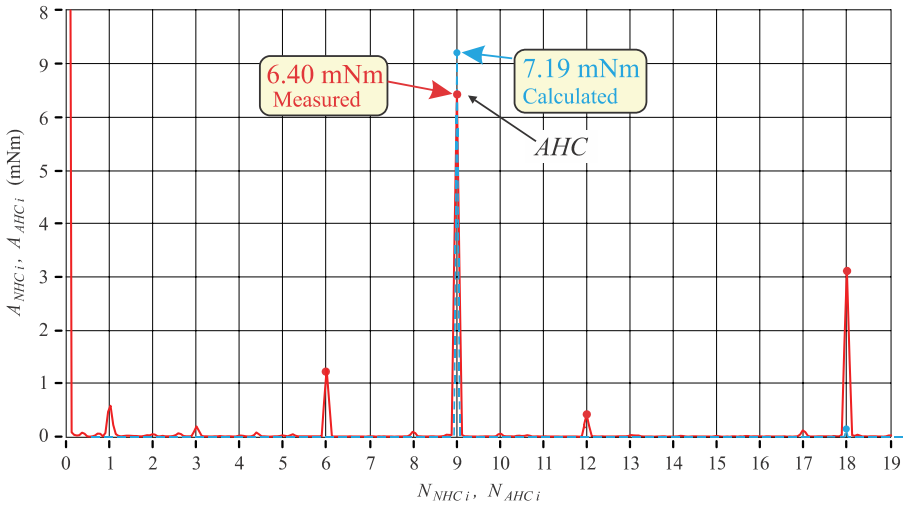

Fig. 13. FFT of T_{cog} – comparison of calculated and measured results

6. Conclusion

Manufacturing assembly imperfections like rotor PMs misplacements cause the phenomena of T_{AHC}, which are not present in the case of an absolutely symmetrical rotor and mostly result in an increased level of total T_{cog}. However it is also possible that the influence of an individual imprecision compensates with others due to different phase shifts which can result even in the decrease of total T_{cog}. Considering the introduced analysis motor designers are able to predict the entire cogging torque harmonic spectrum for any PMSM in advance, thus predetermine required manufacturing tolerances to minimize cogging torque and fulfill the stringent market demands.

References

[1] Gieras J.F., *Permanent-Magnet Motor Technology – Design and Applications.* CRC Press, 3rd edn. (2010).
[2] Krishnan R., *Permanent Magnet Synchronous and Brushless DC Motor Drives*. CRC Press (2010).
[3] Bianchi N., Bolognani S., *Design techniques for reducing the cogging torque in surface-mounted PM motors.* IEEE Transaction on Industry Application 38(5): 1259-1265 (2002).
[4] Islam R., Husain I., Fardoun A., McLaughlin K., *Permanent-magnet synchronous motor magnet designs with skewing for torque ripple and cogging torque reduction*. IEEE Transactions on Industry Applications 45(1): 152-160 (2009).
[5] Islam M.S., Mir S., Sebastian T., *Issues in reducing the cogging torque of mass-produced permanent magnet brushless DC motors.* IEEE Transaction on Industry Application 40(3): 813-820 (2004).
[6] Gašparin L., Černigoj A., Markič S., Fišer R., *Additional cogging torque components in permanent magnet motors due to manufacturing imperfections*. IEEE Transactions on Magnetics 45(3): 1210-1213 (2009).
[7] Miljavec D., Zidarič B., *Eddy current losses in permanent magnets of the BLDC machine.* Compel 26(4): 1095-1104 (2007).
[8] Černigoj A., Gašparin L., Fišer R., *Native and additional cogging torque components of PM synchronous motors – evaluation and reduction.* Automatika 51(2): 157-165 (2010).
[9] Lateb R., Takorabet N., Meibody-Tabar F., Enon J., Sarribouete A., *Design technique for reducing the cogging torque in large surface mounted magnet motors.* Proc. 16th ICEM (CD), Poland, Kraków, 1-6 (2004).
[10] Zhu Z.Q., Ruangsinchaiwanich S., Chen Y., Howe D., *Evaluation of superposition technique for calculating cogging torque in permanent-magnet brushless machines.* IEEE Transactions on Magnetics 42(5): 1597-1603 (2006).
[11] Nemec M., Drobnič K., Nedeljković D., Ambrožič V., *Direct current control of a synchronous machine in field coordinates*, IEEE Trans. Industrial Electronics. 56(10): 4052-4061 (2009).
[12] Gašparin L., Černigoj A., Fišer R., *Phenomena of additional cogging torque components influenced by stator lamination stacking methods in PM motors.* Compel 28(3): 682-690 (2009).
[13] Coenen I., Gracia M.H., Hameyer K., *Influence and evaluation of non-ideal manufacturing process on the cogging torque of a permanent magnet excited synchronous machine.* Compel 30(3): 876-884 (2011).
[14] Heins G., Brown T., Thiele M., *Statistical analysis of the effect of magnet placement on cogging torque in fractional pitch permanent magnet motors.* IEEE Transactions on Magnetics 47(8): 2142-2148 (2011).
[15] Gašparin, L., Černigoj, A. and Fišer R., *Additional cogging torque components due to asymmetry in stator back iron of PM synchronous motors*, Compel, 30(3): 894-905, (2011).

[16] Coenen I., van der Giet M., Hameyer K, *Manufacturing tolerances: estimation and prediction of cogging torque influenced by magnetization faults.* IEEE Transactions on Magnetics 48(5): 1932-1936 (2012).
[17] Bianchinni C., Immovilli F. Lorenzani E., Bellini A., Davoli M, *Review of design solutions for internal permanent-magnet machines cogging torque reduction.* IEEE Transactions on Magnetics 48(10): 2685-2693 (2012).
[18] Azar Z., Zhu Z.Q., Ombach G., *Investigation of torque-speed characteristics and cogging torque of fractional-slot IPM brushless AC machines having alternate slot openings.* IEEE Transactions on Industry Applications 48(3): 903-912 (2012).
[19] Wang D., Wang X., Qiao D., Pei Y., Jung S., *Reducing cogging torque in surface-mounted permanent-magnet motors by nonuniform distributed teeth method*. IEEE Transactions on Magnetics 47(9): 2231-2239 (2011).